Cerebral Cortex, June 2018;28: 1980–1990

doi: 10.1093/cercor/bhx104
Advance Access Publication Date: 11 May 2017
Original Article

ORIGINAL ARTICLE

Chemicogenetic Restoration of the Prefrontal Cortex to Amygdala Pathway Ameliorates Stress-Induced Deficits

Jing Wei[1,2], Ping Zhong[1,2], Luye Qin[1], Tao Tan[1] and Zhen Yan[1,2]

[1]Department of Physiology and Biophysics, School of Medicine and Biomedical Sciences, State University of New York at Buffalo, Buffalo, NY 14214, USA and [2]Medical Research, VA Western New York Healthcare System, Buffalo, NY 14215, USA

Address correspondence to Zhen Yan, Department of Physiology and Biophysics, State University of New York at Buffalo, 124 Sherman Hall, Buffalo, NY 14214, USA. Email: zhenyan@buffalo.edu

Jing Wei and Ping Zhong are contributed equally to this work

Abstract

Corticosteroid stress hormones exert a profound impact on cognitive and emotional processes. Understanding the neuronal circuits that are altered by chronic stress is important for counteracting the detrimental effects of stress in a brain region- and cell type-specific manner. Using the chemogenetic tool, Designer Receptors Exclusively Activated by Designer Drugs (DREADDs), which enables the remote, noninvasive and long-lasting modulation of cellular activity and signal transduction in discrete neuronal populations in vivo, we sought to identify the specific pathways that play an essential role in stress responses. We found that prolonged severe stress induced the diminished glutamatergic projection from pyramidal neurons in prefrontal cortex (PFC) to GABAergic interneurons in basolateral amygdala (BLA), leading to the loss of feedforward inhibition and ensuing hyperexcitability of BLA principal neurons, which caused a variety of behavioral abnormalities. Activating PFC pyramidal neurons with hM3D(Gq) DREADD restored the functional connection between PFC and BLA in stressed animals, resulting in the rescue of recognition memory, normalization of locomotor activity and reduction of aggressive behaviors. Inhibiting BLA principal neurons directly with hM4D(Gi) DREADD also blocked BLA hyperactivity and aggressive behaviors in stressed animals. These results have offered an effective avenue to counteract the stress-induced disruption of circuitry homeostasis.

Key words: amygdala, DREADD, GABA, glutamate, prefrontal cortex, stress

Introduction

In response to chronic stress, stress hormones can produce maladaptive changes that lead to cognitive and emotional disturbances, which precipitates mental disorders like anxiety, depression, schizophrenia, and PTSD (de Kloet et al. 2005; Yehuda and LeDoux 2007; McEwen and Morrison 2013). While several brain regions have been implicated as the important targets of stress hormones, including prefrontal cortex (PFC), amygdala, hippocampus, nucleus accumbens, and locus ceruleus (McEwen 2007; Gold 2015), it remains unclear where in the organization of stress system the initial abnormality arises, and how it spreads to the other loci and form feedback loops to generate exaggerated stress responses (Gold 2015).

PFC, a brain region critical for high-level "executive" functions, such as working memory, attention, decision making, and emotional control (Goldman-Rakic 1995; Davidson et al. 2000; Ridderinkhof et al. 2004), is a key target of stress (Arnsten 2009; Popoli et al. 2011; McEwen and Morrison 2013). Stress exerts profound and complex effects on the synaptic structure and function of PFC, as well as PFC-mediated cognitive processes

(Radley et al. 2006; Liston et al. 2009; Lee et al. 2012; Yuen et al. 2009, 2011, 2012; Wei et al. 2014). Mounting evidence suggests that chronic stress not only impairs cognition, but also induces long-lasting psyco-behavioral changes via altering prefrontal networks (Duman and Aghajanian 2012; Arnsten 2015). To determine the key neuronal circuits underlying the emotional and cognitive deficits induced by prolonged severe stress, we have used an innovative chemogenetic tool, Designer Receptors Exclusively Activated by Designer Drugs (DREADDs).

DREADDs are engineered G-protein coupled receptors that are activated by otherwise inert drug-like ligands. The DREADD encoding the evolved Gq-coupled M3-muscarinic receptor (hM3Dq) or Gi-coupled M4-muscarinic receptor (hM4Di), which is activated by exogenous administration of the small molecule clozapine-N-oxide (CNO), induces neuronal burst firing or neuronal silencing, respectively (Armbruster et al. 2007; Alexander et al. 2009; Rogan and Roth 2011; Garner et al. 2012). These reverse-engineered GPCRs allow the remote, noninvasive, and long-lasting modulation of signal transduction pathways in discrete neuronal populations in vivo (Wess et al. 2013; Urban and Roth 2015). Using this powerful chemicogenetic technology, we sought to find out the specific pathways that play an essential role in stress responses, and to explore novel strategies to reverse the detrimental effects of prolonged stress by normalizing the functional connections.

Methods

Prolonged Severe Stress Paradigm: All experiments were performed with the approval of the Institutional Animal Care and Use Committee (IACUC) of the State University of New York at Buffalo. Sprague Dawley male rats were group-housed in cages with a light/dark cycle. For the prolonged severe stress, animals (starting at 3-week-old) were exposed to 2 unpredictable stressors each day for 14 days. The unpredictable stressors were randomly chosen from 4 choices, including restraint in an air-assessable cylinder (4 h), forced-swim in cold water (15°C, 5 min), elevated platform (30 min), and tilted cage with wet bedding on orbital shaking (45° angle, 100 cycle/min, 1 h). The arrangement of stressors was changed every day in order to avoid habituation.

Viral vectors and Animal Surgery: Adeno-Associated Virus (AAV)8/CaMKIIα-HA-hM3D(Gq)-IRES-mCitrine (3×10^{12} vp/mL) (Yau and McNally 2015) and AAV8/CaMKIIα- hM4D(Gi)-mCherry (4.1×10^{12} vp/mL) were obtained from the UNC Vector Core (University of North Carolina) or Addgene. Stereotaxic injection of the virus (1 μL) to the prelimbic region of PFC or other brain areas was performed as we previously described (Yuen et al. 2011, 2012). In brief, rats were anaesthetized and placed on a stereotaxic apparatus (David Kopf Instruments). The injection was carried out with a Hamilton syringe (needle gauge 31) at a speed of ~0.2 μL/min, and the needle was kept in place for an additional 5 min. The virus was delivered bilaterally to the target area using the following coordinates: PFC, 2.5 mm anterior to bregma; 0.75 mm lateral; and 3.5 mm dorsal to ventral; basolateral amygdala (BLA), −2.2 mm anterior to bregma; 4.4 mm lateral; and 7.4 mm dorsal to ventral; Hippocampus, −3.4 mm anterior to bregma; 1.6 mm lateral; 3.1 mm dorsal to ventral. Animals were allowed to recover for 2 days before the start of the 14-day exposure to stress. Intraperitoneal injection of CNO or saline was given 1 h before behavioral testing or animal euthanization for brain slicing.

Immunohistochemistry: PFC-containing brain slices (100 μm) were collected for 3,3′-diaminobenzidine staining. Endogenous peroxidase activity was first depleted by incubation with hydrogen peroxide. After blocking in 1% bovine serum albumin (Sigma-Aldrich), sections were incubated overnight with the primary antibody against green fluorescent protein (GFP) (1:500, EMD Millipore, AB3080), followed by Vectastain Elite ABC kit (Vector Labs). Sections were imaged with a fluorescent microscope.

Electrophysiological Recordings: Whole-cell patch-clamp experiments were performed with a Multiclamp 700A amplifier and Digidata1322A data acquisition system (Molecular Devices). PFC or amygdala-containing slices were positioned in a perfusion chamber attached to the fixed stage of an upright microscope (Olympus) and submerged in continuously flowing oxygenated artificial cerebrospinal fluid (ACSF) (in mM: 130 NaCl, 26 $NaHCO_3$, 3 KCl, 5 $MgCl_2$, 1.25 NaH_2PO_4, 1 $CaCl_2$, 10 Glucose, pH 7.4, and 300 mOsm). Neurons were visualized with the infrared differential interference contrast video microscopy. Bicuculline (10 μM) and 6-cyano-7-nitroquinoxaline-2,3-dione (25 μM) were added in the recording of *N*-methyl-D-aspartate receptor (NMDAR)-mediated excitatory postsynaptic currents (EPSCs). Bicuculline and D-APV (25 μM) were added in the recording of α-amino-3-hydroxy-5-methyl-4-isoxazolepropionic acid receptor (AMPAR)-mediated EPSC. Patch electrodes contained internal solution (in mM): 130 Cs-methanesulfonate, 10 CsCl, 4 NaCl, 10 HEPES, 1 $MgCl_2$, 5 EGTA, 2.2 QX-314, 12 phosphocreatine, 5 ATP, 0.2 GTP, 0.1 leupeptin, pH 7.2–7.3, and 265–270 mOsm. Evoked EPSC was generated with a pulse from a stimulation isolation unit controlled by a S48 pulse generator (Grass Technologies). A bipolar stimulating electrode (FHC) was placed ~100 μm from the neuron under recording. Tight seals (2–10 GΩ) were obtained by applying negative pressure. The membrane was disrupted with additional suction, and the whole-cell configuration was obtained. Membrane potential was maintained at −70 mV for AMPAR-EPSC recordings. For NMDAR-EPSC, the cell was depolarized to +40 mV for 3 s before stimulation to fully relieve the voltage-dependent Mg^{2+} block. To obtain the input–output responses, EPSC was elicited by a series of stimulation intensities with the same duration of pulses. Recordings from control versus stressed animals were interleaved throughout the course of all experiments.

To record the spontaneous action potential (sAP), slices were bathed in a modified ACSF (in mM: 130 NaCl, 26 $NaHCO_3$, 1 $CaCl_2$, 0.5 $MgCl_2$, 3.5 KCl, 10 glucose, 1.25 NaH_2PO_4) to slightly elevate basal neuronal activity (Yuen et al. 2013; Zhong and Yan 2016), which more closely mimics the ionic composition of brain interstitial fluid in situ (1.0–1.2 mM Ca^{2+}, 1 mM Mg^{2+}, and 3.5 mM K^+) (Sanchez-Vives and McCormic 2000; Maffei et al. 2004). Whole-cell current clamp techniques were used to measure action potential firing with the internal solution containing (in mM: 20 KCl, 100 K-gluconate, 10 HEPES, 4 ATP, 0.5 GTP, and 10 phosphocreatine) (Maffei and Turigiano 2008). A small depolarizing current was applied to adjust the inter-spike potential to −60 mV. The same external and internal solution was used for spontaneous EPSC recordings. Spontaneous inhibitory postsynaptic current (sIPSC) was recorded in regular ACSF with the internal solution (in mM): 100 CsCl, 30 *N*-methyl-D-glucamine, 10 HEPES, 4 NaCl, 1 $MgCl_2$, 5 EGTA, 2 QX-314, 12 phosphocreatine, 5 MgATP, 0.5 Na_2GTP, pH 7.2–7.3, 265–270 mOsM. Data analyses were performed with the Clampfit software (Axon Instruments). Spontaneous synaptic currents were analyzed with Mini Analysis Program (Synaptosoft, Leonia).

To label the neurons under recording, we dialyzed with the internal solution supplemented with 0.05% sulforhodamine B (Invitrogen). Subsequently, slices were fixed with 4% paraformaldehyde for 15 min, then washed 3 time in PBS (pH 7.4). The neuronal images were acquired with a laser scanning confocal microscopy (Carl Zeiss).

Behavioral testing: All behaviors were examined within 3 days after the termination of the prolonged severe stress, and were

carried out during the animals' light cycle. First, animals were subject to the temporal order recognition (TOR) task, as previously described (Yuen et al. 2012; Wei et al. 2014). This task comprised 2 sample phases and 1 test trial. In each sample phase, the animals were allowed to explore 2 identical objects for 3 min. Different objects were used for sample phases I and II, with a 1 h delay between the sample phases. The test trial (3 min) was given 3 h after sample phase II. During the test trial, an object from sample phase I and an object from sample phase II were used. All objects were affixed to a round platform (diameter: 61.4 cm). If TOR memory (TORM) is intact, the animals will spend more time exploring the object from sample I (i.e., the novel object presented less recently). A discrimination ratio (DR), the proportion of time spent exploring the novel versus the familiar object during the test trial was calculated.

Second, the locomotor activity was measured in a rectangular apparatus equipped with photo beam monitors (AccuScan Instruments). Horizontal activity (beam breaks) and total travel distance were recorded during the 10-min test session.

Next, animals were subject to the resident-intruder (RI) test with a modified protocol (Veenema et al. 2006; Márquez et al. 2013). Briefly, each rat was single housed for 24 h before the RI test. Then the resident rat (male) was exposed to an intruder, which was a slightly smaller (5–15% lighter) unfamiliar SD rat (male), in its home cage for 10 min. The attack of the resident rat with the intruder was scored to measure aggression-related behaviors, including the attack latency time, number of attacks, lateral threat, clinch, offensive upright, and keep down. The latter 4 parameters were summarized as total aggressive behavior (Veenema et al. 2006; Márquez et al. 2013).

Statistics: Experiments with 2 groups were analyzed statistically using unpaired Student *t*-tests. Experiments with more than 2 groups were subjected to 1-way or 2-way analysis of variance (ANOVA), followed by Bonferroni post hoc tests.

Results

Chemicogenetic Activation of PFC Pyramidal Neurons Restores Glutamatergic Transmission of PFC in Animals Exposed to Prolonged Severe Stress

To determine whether activating PFC pyramidal neurons could reverse the detrimental effects of prolonged severe stress, we injected a mCitrine-tagged CaMKII-driven Gq-coupled DREADD AAV (Fortress et al. 2015; Yau and McNally 2015; López et al. 2016), hM3D(Gq), into the prelimbic area of PFC, to selectively elevate the excitability of PFC pyramidal neurons. The robust expression of hM3Dq in medial PFC (mPFC) pyramidal neurons was demonstrated by immunoreactivity with the GFP antibody (Fig. 1A). We further performed patch-clamp electrophysiological experiments to functionally validate the chemicogenetic activation of PFC pyramidal neurons. In vivo administration of CNO (3 mg/kg, i.p.) to control rats led to the significantly increased frequency of sAPs in hM3Dq-expressing PFC neurons (Fig. 1B, saline: 1.1 ± 0.2 Hz, $n = 10$ cells, CNO: 1.9 ± 0.3 Hz, $n = 9$ cells, $P < 0.05$, *t*-test), confirming that hM3Dq DREADD system was capable of elevating the activity of PFC pyramidal neurons (Garner et al. 2012; Michaelides et al. 2013).

Next, we measured AMPAR- and NMDAR-mediated EPSC in control versus stressed animals (with prior infection of hM3Dq AAV in PFC) injected with CNO or saline. As shown in Figure 1C,D, compared with control animals (control+saline), stressed animals (stress+saline) had the significantly reduced AMPAR-EPSC and NMDAR-EPSC amplitudes (AMPA: 48%-53% decrease, n = 10–20 per group, $F_{3,55\ (group)} = 6.3$, $P < 0.001$, $F_{4,220\ (stimulation)} = 129.1$, $P < 0.001$, $F_{12,220\ (interaction)} = 4.8$, $P < 0.001$, 2-way rmANOVA; NMDA: 40–47% decrease, n = 9–14 per group, $F_{3,42\ (group)} = 7.2$, $P < 0.001$, $F_{4,168\ (stimulation)} = 199.8$, $P < 0.001$, $F_{12,168\ (interaction)} = 5.4$, $P < 0.001$, 2-way rmANOVA), which was restored by CNO activation of hM3Dq DREADD (stress+CNO) (AMPA: $n = 10$; NMDA: $n = 9$, $P > 0.05$, compared with control+saline). CNO administration to the control group (control+CNO) did not significantly alter the amplitude of AMPAR-EPSC and NMDAR-EPSC (AMPA: $n = 13$; NMDA: $n = 10$, $P > 0.05$, compared with control+saline). These results suggest that prolonged severe stress produces a sustained down-regulation of glutamatergic transmission in the PFC, and chemicogenetic activation of PFC pyramidal neurons leads to the rescue of synaptic deficits in stressed animals.

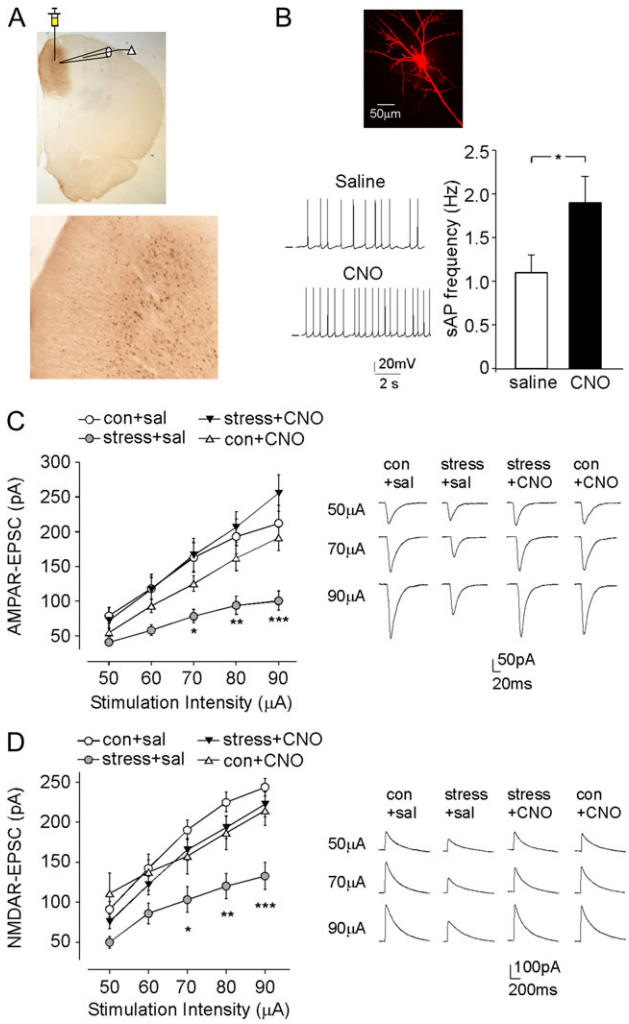

Figure 1. DREADD-based activation of PFC pyramidal neurons rescues PFC glutamatergic signaling in rats exposed to prolonged severe stress. (*A*) Images (1× and 4×) of GFP staining showing the location and expression of the stereotaxically injected CaMKIIα-hM3D(Gq)-mCitrine AAV to the medial PFC region. (*B*) Representative spontaneous AP (sAP) traces and bar graph summary of sAP frequencies in PFC pyramidal neurons from saline versus CNO (3 mg/kg, i.p)-injected control rats infected with hM3Dq. *$P < 0.05$, *t*-test. Inset: A representative layer V PFC pyramidal neuron used for recording. (*C*, *D*) Summarized input–output curves of AMPAR-EPSC (*C*) and NMDAR-EPSC (*D*) in layer V PFC pyramidal neurons from control (con) versus stressed (exposed to 2-week unpredictable severe stress) rats (with prior infection of hM3Dq AAV in PFC) injected with saline or CNO. ***$P < 0.001$, **$P < 0.01$, *$P < 0.05$, 2-way ANOVA. Inset: representative AMPAR-EPSC or NMDAR-EPSC traces.

Chemicogenetic Activation of PFC Pyramidal Neurons Rescues Behavioral Deficits in Animals Exposed to Prolonged Severe Stress

Since chemicogenetic activation of PFC pyramidal neurons rescued the synaptic output of PFC in stressed animals, we further tested whether it could reverse stress-induced behavioral abnormalities. First, the TORM, a PFC-mediated memory process requiring judgments of the prior occurrence of stimuli based on the recency and relative familiarity information (Barker et al. 2007), was measured. As shown in Figure 2A, control animals (control+saline) spent significantly more time exploring the novel (less recent) object than the familiar object (novel object: 19.9 ± 1.8 sec, familiar object: 9.3 ± 0.8 s, $n = 6$, $P < 0.01$, t-test), and stressed rats (stress+saline) lost the preference to the novel object (novel object: 15.0 ± 2.9 s, familiar object: 15.2 ± 2.9 s, $n = 6$, $P > 0.05$, t-test), while CNO activation of hM3Dq in PFC (stress+CNO) reversed the loss (novel object: 13.0 ± 1.4 sec, familiar object: 6.5 ± 0.3 s, $n = 4$, $P < 0.05$, t-test). The DR, an index of the object recognition memory, indicated a profound impairment of TORM by prolonged severe stress, which was rescued after CNO activation of hM3Dq in PFC (3 mg/kg, i.p. at 5–7 day after stress cessation, Fig. 2B, control+saline: 36.2 ± 2.9%, $n = 6$; stress+saline: −0.4 ± 3.5%, $n = 6$; stress+CNO: 32.4 ± 5.3%, $n = 4$; control+CNO: 31.5 ± 8.4%, $n = 5$; $F_{1,17\ (animal)} = 11.8$, $P < 0.01$, $F_{1,17\ (treatment)} = 7.3$, $P < 0.05$, $F_{1,17\ (interaction)} = 12.9$, $P < 0.01$, 2-way ANOVA).

In addition, rats exposed to prolonged severe stress exhibited the significantly increased locomotive activity, which was also reversed by CNO activation of hM3Dq in PFC (Fig. 2C, horizontal activity, control+saline: 2319.1 ± 215.1, $n = 9$; stress+saline: 3511.3 ± 199.5, $n = 9$; stress+CNO: 2149.0 ± 383.8, $n = 7$, control+CNO: 2075.7 ± 138.7, $n = 6$; $F_{1,27\ (animal)} = 6.3$, $F_{1,27\ (treatment)} = 10.1$, $F_{1,27\ (interaction)} = 4.9$, $P < 0.05$, 2-way ANOVA; total distance, control+saline: 1032.5 ± 92.7 cm, $n = 9$; stress+saline: 1888.0 ± 155.6 cm, $n = 9$; stress+CNO: 1084.1 ± 206.0 cm, $n = 7$; control+CNO: 956.3 ± 144.6 cm, $n = 6$; $F_{1,27\ (animal)} = 10.3$, $F_{1,27\ (treatment)} = 8.2$, $F_{1,27\ (interaction)} = 5.6$, $P < 0.05$, 2-way ANOVA).

Furthermore, stressed animals exhibited more aggression-like behaviors in RI tests, as demonstrated by the significantly increased attack numbers (Fig. 2D, control+saline: 7.0 ± 1.8, $n = 6$; stress+saline: 17.0 ± 2.4, $n = 6$, $F_{1,21\ (animal)} = 6.4$, $P < 0.05$, 2-way ANOVA) and attack durations (control+saline: 36.6 ± 8.7 s, $n = 6$; stress+saline: 102.9 ± 12.9 s, $n = 6$, $F_{1,21\ (animal)} = 10.0$, $P < 0.01$, 2-way ANOVA). However, stressed animals with DREADD-mediated activation of mPFC by CNO injection showed the decreased attack numbers (stress+CNO: 8.0 ± 2.1, $n = 7$; control+CNO: 8.0 ± 1.4, $n = 6$; $F_{1,21\ (treatment)} = 4.1$, $P < 0.05$, $F_{1,21\ (interaction)} = 6.4$, $P < 0.05$, 2-way ANOVA) and attack durations (stress+CNO: 49.5 ± 15.0 s, $n = 7$; control+CNO: 42.9 ± 4.5 s, $n = 6$; $F_{1,21\ (treatment)} = 4.2$, $P < 0.05$, $F_{1,21\ (interaction)} = 6.7$, $P < 0.05$, 2-way ANOVA) in RI tests. These results suggest that prolonged severe stress produces a variety of behavioral changes, including the loss of recognition memory, hyperactivity and increased aggression, and chemicogenetic activation of PFC pyramidal neurons is capable of rescuing these behavioral deficits in stressed animals.

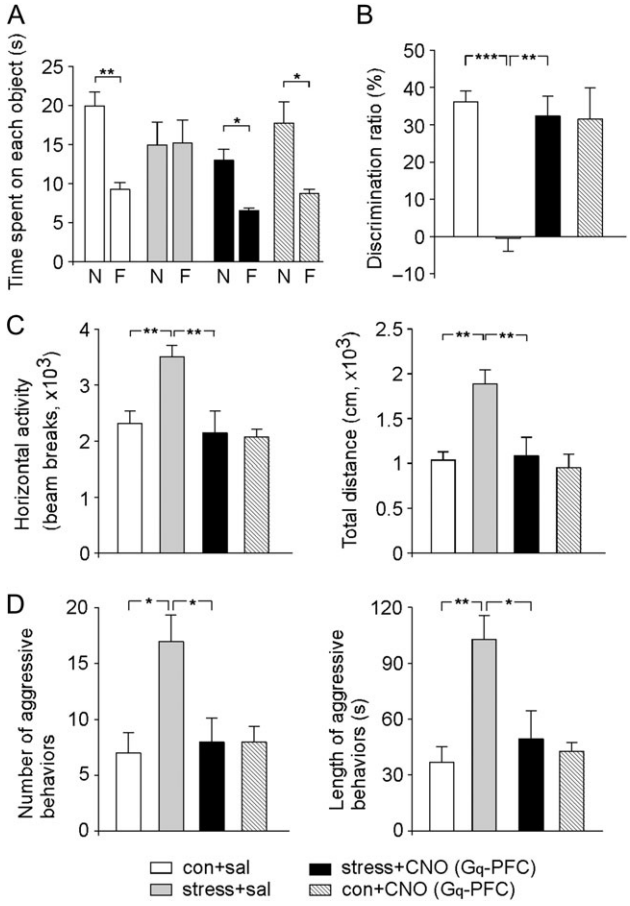

Figure 2. DREADD-based activation of PFC pyramidal neurons reverses behavioral deficits in rats exposed to prolonged severe stress. (*A*, *B*) Bar graphs (mean ± SEM) showing the exploration time of novel versus familiar objects (*A*) and DR (*B*) of TORM task in control versus stressed rats (with prior delivery of hM3Dq AAV to PL) injected with saline or CNO.***$P < 0.001$, **$P < 0.01$, *$P < 0.05$, ANOVA. Inset (*A*): an image showing the location of DREADD delivery. (*C*) Bar graphs (mean ± SEM) showing the horizontal activity and the total travel distance of locomotion tests in control versus stressed rats (with prior delivery of hM3Dq AAV to PL) injected with saline or CNO. **$P < 0.01$, ANOVA. (*D*) Bar graphs (mean ± SEM) showing the number and durations of attacks in the RI test for aggression measurements in control versus stressed rats (with prior delivery of hM3Dq AAV to PL) injected with saline or CNO. **$P < 0.01$, *$P < 0.05$, ANOVA.

Chemicogenetic Activation of PFC Pyramidal Neurons Rescues GABAergic Transmission of BLA in Animals Exposed to Prolonged Severe Stress

Next, we sought to determine the role of PFC projecting regions in the stress responses. The hM3Dq DREADD that infects PFC pyramidal neurons should be able to traffic axonally, influencing neurons in the projecting regions. One of the PFC projecting areas that may control the stress-induced changes is amygdala. Anatomic studies have found that the prelimbic cortex (PL) has abundant projections to the BLA (McDonald et al. 1996). Immunohistochemical results have also demonstrated that viruses injected into the principal neurons of PL can spread to the axonal terminals in BLA (Cho et al. 2013; Huang et al. 2016).

To find out the functional connectivity between PL and BLA, we first examined whether activating PL axon terminals in BLA by local CNO application could alter the synaptic strength and excitability of amygdala neurons. One major neuronal type in amygdala is the large pyramidal principal neuron (Fig. 3A). Using control rats injected with hM3Dq AAV to PL, we found that bath application of CNO to BLA induced a significant decrease of the excitability of BLA principal neurons, as demonstrated by the reduced frequency of sAP (baseline: 1.35 ± 0.26 Hz; +CNO: 0.92 ± 0.15 Hz, $n = 6$, $P < 0.05$, t-test). A representative neuron is shown

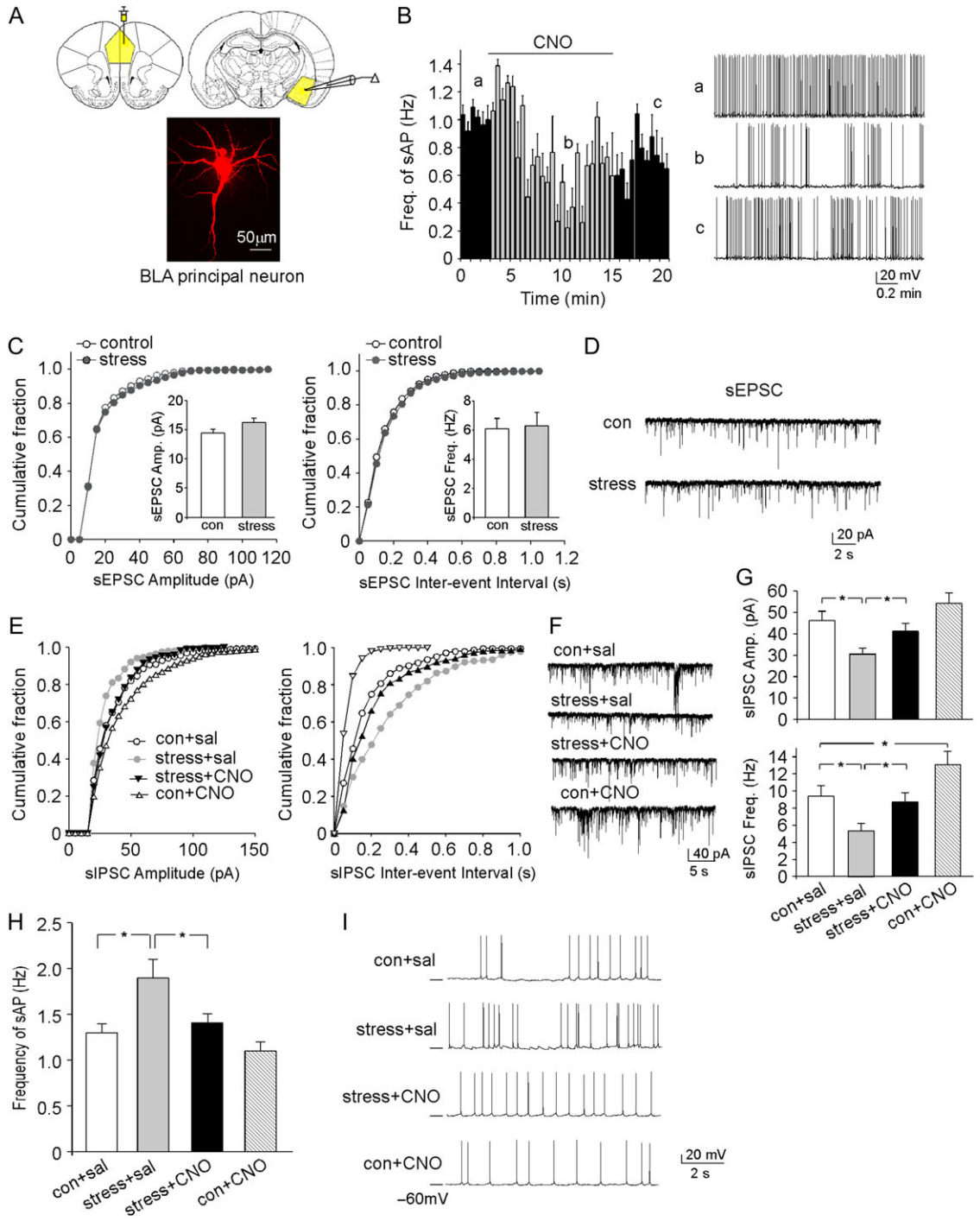

Figure 3. DREADD-based activation of PFC pyramidal neurons normalizes the GABAergic response and excitability of BLA principal neurons in rats exposed to prolonged severe stress. (*A*) Image of a BLA principal neuron. Inset: an image showing the location of DREADD delivery and electrophysiological recordings. (*B*) Plot of sAP frequencies before (con), during (CNO), and after (wash) bath application of CNO (5 μM) in a BLA principal neuron from a control rat with PL injection of hM3Dq AAV. Inset: representative sAP traces at different time points designated as a, b, c on the time course plot. (*C*) Cumulative distribution of sEPSC amplitudes and inter-event intervals in BLA principal neurons from a control rat versus a rat exposed to 2-week unpredictable severe stress. Inset: bar graphs (mean ± SEM) of sEPSC amplitude and frequency in BLA principal neurons from control versus stressed rats. (*D*) Representative sEPSC traces. (*E*) Cumulative distribution of sIPSC amplitudes and inter-event intervals in BLA principal neurons from control versus stressed rats (with prior delivery of hM3Dq AAV to PL) injected with saline or CNO. (*F*) Representative sIPSC traces. (*G*) Bar graphs (mean ± SEM) of sIPSC amplitude and frequency in BLA principal neurons from different groups. *$P < 0.05$, ANOVA. (*H*) Bar graphs (mean ± SEM) showing the synaptic-driven sAP frequency in BLA principal neurons from control vs. stressed rats (with prior delivery of hM3Dq AAV to PL) injected with saline or CNO. *$P < 0.05$, ANOVA. (*I*) Representative sAP traces.

in Figure 3*B*. It suggests that chemicogenetic activation of the terminals of PFC pyramidal neurons in BLA leads to inhibition of BLA principal neurons.

To test the impact of stress-induced PFC dysfunction on BLA, we examined synaptic responses in BLA principal neurons from control versus stressed animals. As shown in Figure 3*C*,*D*,

no significant alteration was found on the amplitude and frequency of spontaneous excitatory postsynaptic currents (sEPSCs) in BLA principal neurons from rats exposed to prolonged severe stress (control: 14.4 ± 0.7 pA, 6.1 ± 0.7 Hz, $n = 13$, stress: 16.2 ± 0.8 pA, 6.3 ± 0.9 Hz, $n = 14$, $P > 0.05$, t-test). In contrast, the amplitude and the frequency of sIPSCs were significantly reduced in BLA principal neurons from stressed animals (Fig. 3E–G, con+saline: 46.2 ± 4.1 pA, 9.4 ± 1.2 Hz, $n = 8$, stress+saline: 30.3 ± 2.3 pA, 5.3 ± 0.9 Hz, $n = 10$, $F_{1,29\ (animal)} = 10.6$ (amp), $F_{1,29\ (animal)} = 13.8$ (freq), $P < 0.01$, 2-way ANOVA). CNO activation of hM3Dq in PFC rescued the diminished sIPSC in BLA principal neurons from stressed animals (stress+CNO: 41.9 ± 3.1 pA, 8.7 ± 1.1 Hz, $n = 8$, $F_{1,29\ (treatment)} = 4.4$ (amp), $F_{1,29\ (treatment)} = 9.6$ (freq), $P < 0.05$, 2-way ANOVA).

Measurements of the synaptic-driven sAPs showed that the frequency of sAP was significantly increased in BLA principal neurons by prolonged severe stress, which was reversed by CNO activation of hM3Dq in PFC (Fig. 3H,I, con+sal: 1.3 ± 0.1 Hz, $n = 6$, stress+sal: 1.9 ± 0.2 Hz, $n = 8$, stress+CNO: 1.4 ± 0.1 Hz, $n = 7$, con+CNO: 1.1 ± 0.1 Hz, $n = 7$, $F_{1,24\ (animal)} = 8.9$, $P < 0.01$, $F_{1,24\ (treatment)} = 4.7$, $P < 0.05$, 2-way ANOVA). Taken together, these results suggest that stress induces the disinhibition and hyperexcitability of BLA principal neurons, which can be rescued by the chemicogenetic activation of PFC projection neurons.

To further demonstrate that the stress-induced hyperexcitability of BLA principal neurons is due to the loss of feedforward inhibition, we directly measured BLA interneurons. Morphological studies have found intense GABA-positive staining in the amygdala, suggesting that many amygdala neurons are GABAergic (McDonald 1982; Savander et al. 1996; Spampanato et al. 2011). As shown in Figure 4A, BLA interneurons have the much smaller soma size and the multipolar soma shape, which can be easily distinguished from BLA principal neurons. Other than the morphological differences, BLA interneurons also exhibit different electrophysiological features, compared with BLA principal neurons (Table 1). Particularly, the sEPSC of BLA interneurons has significantly bigger amplitude (~2.0 fold) and faster decay kinetics (~3.7 fold), and the sAP of BLA interneurons has significantly higher frequency (~6.7-fold).

To test the impact of stress on BLA interneurons, we first examined their synaptic responses to glutamatergic inputs. As shown in Figure 4B, sEPSC amplitude and frequency were significantly reduced in BLA interneurons from rats exposed to prolonged severe stress, and CNO activation of hM3Dq in PFC rescued the diminished sEPSC in BLA interneurons from stressed animals (control+saline: 40.3 ± 2.6 pA, 10.6 ± 0.8 Hz, $n = 9$, stress+saline: 29.6 ± 1.3 pA, 7.5 ± 0.4 Hz, $n = 10$, stress+ CNO: 38.9 ± 2.1 pA, 10.4 ± 0.7 Hz, $n = 10$, control+CNO: 41.6 ± 3.1 pA, 11.4 ± 1.0 Hz, $n = 10$, $F_{1,35\ (animal)} = 5.0$ (amp), $F_{1,35\ (animal)} = 5.5$ (freq),

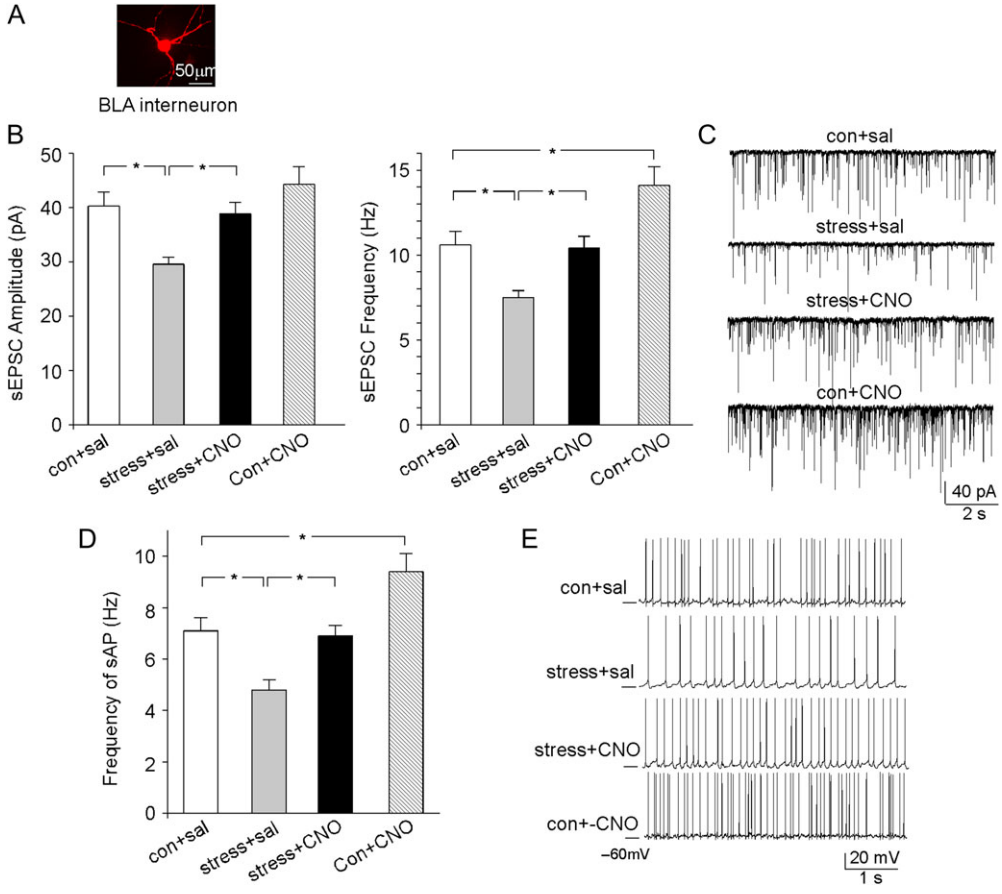

Figure 4. DREADD-based activation of PFC pyramidal neurons restores the glutamatergic response and excitability of BLA interneurons in rats exposed to prolonged severe stress. (*A*) Images of a BLA small GABAergic interneuron. (*B*) Bar graphs of sEPSC amplitudes and frequencies in BLA interneurons from control versus stressed rats (with prior delivery of hM3Dq AAV to PL) injected with saline or CNO. *$P < 0.05$, ANOVA. (*C*) Representative sEPSC traces in BLA interneurons from different groups. (*D*) Bar graphs (mean ± SEM) showing the synaptic-driven sAP frequency in BLA interneurons from control versus stressed rats (with prior delivery of hM3Dq AAV to PL) injected with saline or CNO. *$P < 0.05$, ANOVA. (*E*) Representative sAP traces in BLA interneurons from different groups.

Table 1. Comparison of electrophysiological measurements of BLA principal neurons and BLA interneurons

	BLA principal neuron ($n = 7$)	BLA interneuron ($n = 7$)
Cm (pF)	69.8 ± 3.9	34.6 ± 2.0*
sEPSC		
Amplitude (pA)	19.7 ± 1.3	38.8 ± 2.7*
Frequency (Hz)	9.4 ± 0.7	10.7 ± 0.8
Decay time constant (ms)	10.7 ± 0.8	2.9 ± 0.3**
sAP frequency (Hz)	1.12 ± 0.27	7.48 ± 0.52**

Cm, membrane capacitance; *$P < 0.01$; **$P < 0.001$, *t*-test.

$F_{1,35\ (treatment)} = 8.1$ (amp), $F_{1,35\ (treatment)} = 6.8$ (freq), $P < 0.05$, 2-way ANOVA). Moreover, the synaptic-driven sAP frequency was significantly decreased in BLA interneurons by prolonged severe stress, which was reversed by CNO activation of hM3Dq in PFC (Fig. 4C, con+sal: 7.1 ± 0.5 Hz, $n = 9$, stress+sal: 4.8 ± 0.4 Hz, $n = 10$, stress+CNO: 6.9 ± 0.5 Hz, $n = 10$, con+CNO: 9.3 ± 0.7 Hz, $n = 10$, $F_{1,35\ (animal)} = 22.5$, $F_{1,35\ (treatment)} = 20.1$, $P < 0.001$, 2-way ANOVA). These results suggest that the stress-induced reduction of glutamatergic input from PFC to BLA interneurons has caused the loss of BLA interneuron excitability, which can be rescued by the chemicogenetic activation of PFC projection neurons.

Chemicogenetic Suppression of BLA Principal Neurons Blocks the Stress-Induced BLA Hyperactivity and Aggressive Behaviors

Since chemicogenetic activation of PFC pyramidal neurons blocked the stress-induced hyperexcitability of BLA principal neurons and behavioral deficits, we would like to know whether the direct suppression of BLA principal neuronal activity could have the same outcome. To test this, we injected the mCherry-tagged CaMKII-driven Gi-coupled DREADD AAV (Krashes et al. 2011; Rogan and Roth 2011), hM4D(Gi), into the BLA region to selectively dampen the excitability of BLA principal neurons. The delivery and expression of hM4D(Gi) AAV in BLA is shown in Figure 5A.

We first performed electrophysiological experiments to functionally validate the chemicogenetic suppression of BLA activity. In hM4Di-expressing BLA principal neurons, bath application of CNO (5 μM) induced the silencing of sAPs (Fig. 5B, $n = 6$), while no such effect was observed in uninfected neighboring neurons (Fig. 5B, $n = 5$), suggesting that the hM4Di DREADD system was capable of suppressing BLA output.

Next, we delivered hM4Di AAV to BLA, and measured the excitability of BLA principal neurons from control versus stressed animals injected with CNO or saline. As shown in Figure 5C, compared with saline-injected control rats (con+sal), saline-injected stressed rats (stress+sal) had a significantly higher frequency of sAP, which was reversed by CNO activation of hM4Di in BLA of stressed animals (stress+CNO), and CNO administration to control rats (con+CNO) also led to the significantly decreased sAP frequency in BLA (con+sal: 1.2 ± 0.1 Hz, $n = 12$, stress+sal: 1.8 ± 0.2 Hz, $n = 9$, stress+CNO: 1.1 ± 0.2 Hz, $n = 8$, con+CNO: 0.8 ± 0.1 Hz, $n = 11$, $F_{1,36\ (animal)} = 23.3$, $P < 0.001$, $F_{1,36\ (treatment)} = 11.3$, $P < 0.01$, 2-way ANOVA). It suggests that chemicogenetic inhibition of BLA principal neurons can reverse the stress-induced hyperactivity of these neurons.

Moreover, we measured various behaviors in stressed animals with chemicogenetic suppression of BLA activity. Since PL projects to several brain regions other than BLA, such as hippocampus, we also directly manipulated hippocampal activity with the chemicogenetic tool and examined behavioral changes. In the TORM test, the stress-induced loss of the preference to the novel object was not reversed by either CNO activation of hM4Di in BLA or CNO activation of hM3Dq in hippocampus (Fig. 6A), as reflected in the impaired DR in stressed animals (Fig. 6B, control+saline: 32.3 ± 7.5%, $n = 9$; stress+saline: −3.0 ± 4.1%, $n = 9$; stress+CNO (BLA): −4.1 ± 8.6%, $n = 5$, stress+CNO (Hip): −7.5 ± 10.6%, $n = 5$; $F_{3,24} = 7.4$, $P < 0.01$, 1-way ANOVA). It suggests that TORM requires the normal activity of neural circuits upstream of BLA or hippocampus.

In the locomotion test, the stress-induced increase of locomotive activity was normalized by either CNO activation of hM4Di in BLA or CNO activation of hM3Dq in hippocampus (Fig. 6C, horizontal activity/total distance, control+saline: 2870.0 ± 198.1/1155.0 ± 96.5 cm, $n = 9$; stress+saline: 3893.0 ± 61.3/1699.0 ± 90.3 cm, $n = 7$; stress+CNO (BLA): 2910.0 ± 219.9/1201.0 ± 115.0 cm, $n = 5$, stress+CNO (Hip): 2356.0 ± 324.0/931.4 ± 152.5 cm, $n = 5$; $F_{3,22} = 9.4$ (horizontal activity), $F_{3,22} = 8.4$ (total distance), $P < 0.001$, 1-way ANOVA). It suggests that locomotion is controlled by diverse pathways involving multiple brain regions.

In RI tests, the stress-induced increase of aggressive behaviors was significantly reduced by CNO activation of hM4Di in BLA, but not by CNO activation of hM3Dq in hippocampus (Fig. 6D, attack numbers/attack durations, control+saline: 11.6 ± 0.9/37.1 ± 3.7 s, $n = 11$; stress+saline: 18.4 ± 1.1/78.0 ± 4.8 s, $n = 14$; stress+CNO (BLA): 9.8 ± 1.0/40.0 ± 5.8 s, $n = 8$, stress+CNO (Hip): 15.6 ± 0.7/71.7 ± 9.4 s, $n = 5$, $F_{3,34} = 15.1$ (attack number), $F_{3,34} = 17.6$ (attack duration), $P < 0.001$, 1-way ANOVA). Taken together, these data suggest that chemicogenetic inhibition of BLA principal neurons can reverse some of the stress-induced behavioral changes, such as the increased aggression.

Discussion

Using the DREADD-based strategy, which has the capability to precisely control long-range and local neural network (Alexander et al. 2009; Michaelides et al. 2013; Wess et al. 2013; Urban and Roth 2015), we have come up with the following model regarding the stress-induced alteration of neuronal circuits (Fig. 7). Prolonged severe stress induces the diminished glutamatergic projection from PFC pyramidal neurons to BLA GABAergic interneurons, leading to the loss of feedforward inhibition and ensuing hyperexcitability of BLA principal neurons, which causes a variety of behavioral abnormalities. Activating PFC pyramidal neurons with DREADD rescues the functional connection between PFC and BLA in stressed animals, resulting in the restoration of recognition memory, normalization of locomotor activity and reduction of aggressive behaviors. Inhibiting BLA principal neurons directly with DREADD also blocks BLA hyperactivity and aggressive behaviors in stressed animals.

Convergent evidence from primate and human studies indicates that the adaptive goal-directed and self-regulated behaviors elicit largely overlapping clusters of activation foci in medial frontal cortex (Ridderinkhof et al. 2004), suggesting the central role of PFC in cognitive control. Prefrontal synaptic abnormalities have been strongly associated with cognitive and emotional dysfunction in a variety of mental disorders (Kim et al. 2010; Krueger et al. 2011; Duffney et al. 2015). Behavioral stress affects both the structure and function of PFC over the life course

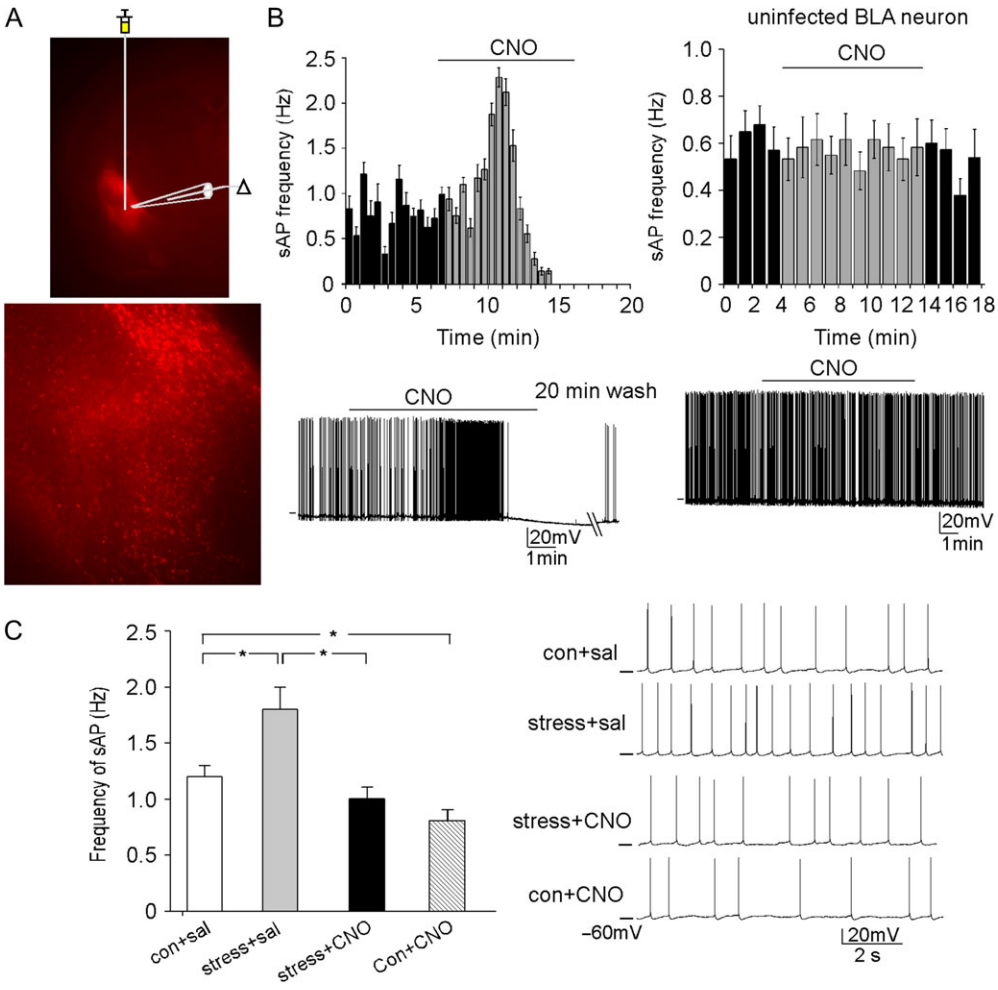

Figure 5. DREADD-based inhibition of BLA principal neurons normalizes the BLA neuronal excitability in rats exposed to prolonged severe stress. (*A*) Fluorescent images (1× and 4×) showing the location and expression of the stereotaxically injected CaMKIIα-hM4D(Gi)-mCherry AAV to the BLA region. (*B*) Plot of sAP frequencies before and after bath application of CNO (5 μM) in representative hM4Di-positive and hM4Di-negative (uninfected) BLA principal neurons from rats with BLA injection of hM4Di AAV. Inset: Representative sAP traces. (*C*) Bar graphs (mean ± SEM) showing sAP frequencies in BLA principal neurons from control vs. stressed rats (with prior delivery of hM4Di AAV to BLA) injected with saline or CNO. *$P < 0.05$, ANOVA. Inset: Representative sAP traces.

(McEwen and Morrison 2013), with glutamatergic synapses in PFC neurons as the major target of corticosteroid stress hormones (Popoli et al. 2011). Exposure to repeated or chronic unpredictable stress decreases the expression of synaptic proteins and excitatory synaptic currents in PFC pyramidal neurons (Li et al. 2011; Yuen et al. 2012). New treatment to reverse the behavioral and neuronal deficits of chronic stress and depression is focusing on glutamate and synaptic plasticity (Duman and Aghajanian 2012; Gerhard et al. 2016). However, pharmacological avenues often lack the brain region and cell type specificity.

In recent years, DREADD has emerged as a novel and powerful tool to investigate discrete neuronal populations with therapeutic utility (Wess et al. 2013; Urban and Roth 2015). Compared with opotogenetic approaches, this chemicogenetic method has the advantages of being less invasive and having more sustained effects. Using DREADD to selectively activate PFC pyramidal neurons in animals exposed to prolonged severe stress, we have observed the restoration of glutamatergic transmission in PFC, suggesting that the output of PFC can be normalized by this chemicogenetic approach.

PFC projects to multiple subcortical regions that may contribute to the stress-induced behavioral deficits (McEwen 2007; Gold 2015). Using anterograde tract tracing, it has been found that each of the rat PFC subregions (prelimbic, intralimbic, and cingulate) has a distinctive projection to the amygdala, with PL mainly projecting to BLA (McDonald et al. 1996). BLA projects to central amygdala, which provides the major output of the amygdala complex to control fear and emotional responses. Using DREADD to activate PL axon terminals in BLA, we have observed the reduced excitability of BLA principal neurons, suggesting that the glutamatergic output of PFC may directly activate BLA GABAergic interneurons, resulting in feedforward inhibition of BLA principal neurons. Consistently, in vivo intracellular recordings demonstrate that PFC stimulation inhibits BLA projection neurons, which is attributable to the recruitment of inhibitory interneurons (Rosenkranz and Grace 2002). In rats exposed to prolonged severe stress, the diminished PFC activation of BLA interneurons leads to the decreased GABAergic inputs and disinhibition of BLA principal neurons. Weakened prefrontal cortical modulation of amygdala neuronal activity by chronic cold stress has also been found in in vivo extracellular recordings (Correll et al. 2005). Importantly, the functional connection between PFC and BLA of stressed animals is normalized by DREADD activation of PFC pyramidal neurons. Thus, restoring the PFC-mediated

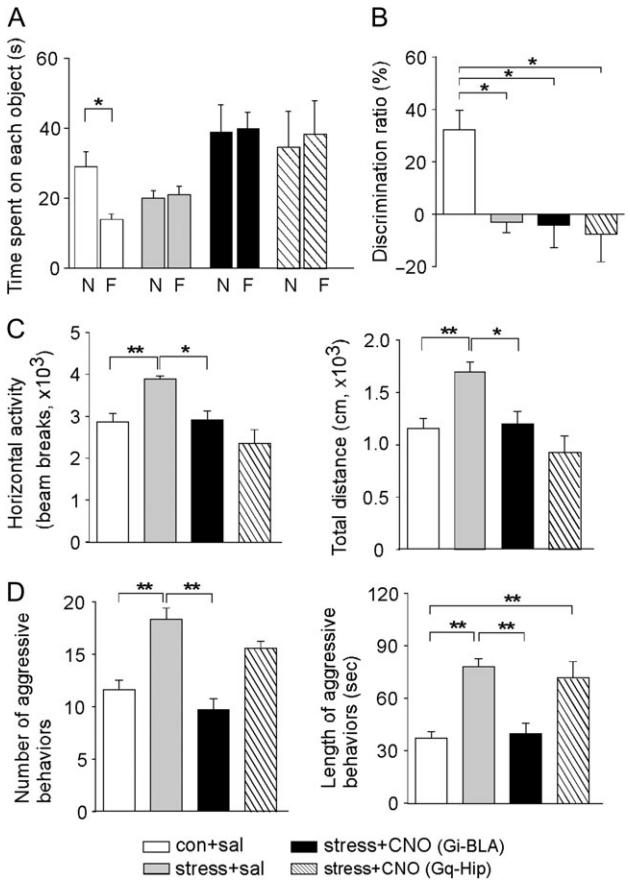

Figure 6. DREADD-based inhibition of BLA principal neurons reverses some behavioral deficits in rats exposed to prolonged severe stress. (*A*, *B*) Bar graphs (mean ± SEM) showing the exploration time of novel versus familiar objects (*A*) and DR (*B*) of TORM task in control versus stressed rats (with prior delivery of hM4Di AAV to BLA or hM3Dq AAV to Hip) injected with saline or CNO. $^{*}P < 0.05$, ANOVA. (*C*) Bar graphs (mean ± SEM) showing the horizontal activity and the total travel distance of locomotion tests in control versus stressed rats (with prior delivery of hM4Di AAV to BLA or hM3Dq AAV to Hip) injected with saline or CNO. $^{**}P < 0.01$, $^{*}P < 0.05$, ANOVA. (*D*) Bar graphs (mean ± SEM) showing the number and durations of attacks in the RI test for aggression measurements in control versus stressed rats (with prior delivery of hM4Di AAV to BLA or hM3Dq AAV to Hip) injected with saline or CNO. $^{**}P < 0.01$, ANOVA.

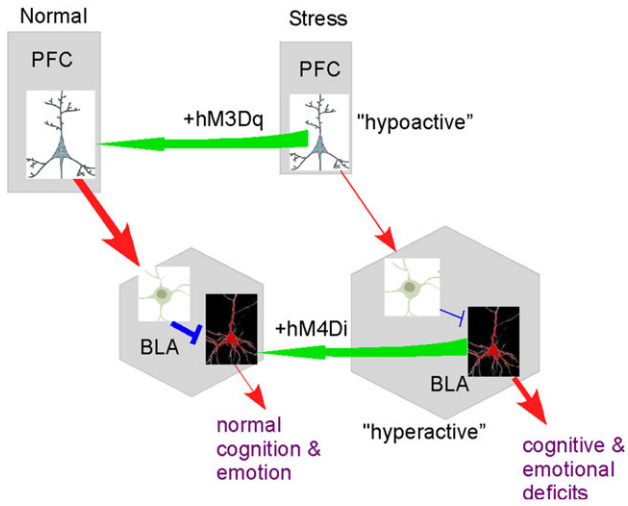

Figure 7. A schematic diagram showing the alterations in the neuronal circuits by prolonged severe stress and the rescue by DREADD-based activation of functional connections. A PFC pyramidal projection neuron, a BLA GABAergic interneurons and a BLA principal neuron are shown. The thickness of lines indicates the strength of the connection (Red, glutamatergic excitatory link; Blue, GABAergic inhibitory link).

inhibitory control of amygdala offers an effective avenue to counteract the stress-induced disruption of the homeostatic set point of neuronal circuits.

It has been postulated that the impaired PFC function after stress exposure leads to the disinhibition of amygdala, therefore, promoting anxiety and physiological hyperarousal (Gold 2015). Recent studies using mice with cell type-specific knockout of glucocorticoid receptors have found that forebrain glutamatergic, but not GABAergic, neurons mediate fear and anxiety behaviors (Hartmann et al. 2017). Our behavioral assays of animals exposed to prolonged severe stress have found the loss of PFC-mediated cognitive function, which is likely attributable to the diminished function of PFC glutamatergic neurons. In addition, we have found the increased aggression in animals exposed to prolonged severe stress, which is likely attributable to the disinhibition of BLA principal neurons. Indeed, impulsive aggression and violence is thought to arise as a consequence of faulty emotion regulation because of dysfunctional PFC and its connected neural circuitry (Davidson et al. 2000). Stressed individuals vulnerable to dysregulation of negative emotion are at risk for violence and aggression (Tielbeek et al. 2016; Waltes et al. 2016). Interestingly, the behavioral abnormalities in stressed animals are reversed by DREADD activation of PFC pyramidal neurons or DREADD inhibition of BLA principal neurons, suggesting that the chemicogenetic approach holds promise for the treatment of stress-related mental disorders associated with PFC network dysfunction.

Funding

National Institutes of Health (MH108842 and DA037618); Nancy Lurie Marks Family Foundation and E. F. Trachtman to Z.Y.

Notes

We thank Xiaoqing Chen and Kaijie Ma for the excellent technical support. *Conflict of Interest*: None declared.

References

Alexander GM, Rogan SC, Abbas AI, Armbruster BN, Pei Y, Allen JA, Nonneman RJ, Hartmann J, Moy SS, Nicolelis MA, et al. 2009. Remote control of neuronal activity in transgenic mice expressing evolved G-protein coupled receptors. Neuron. 63: 27–39.

Armbruster BN, Li X, Pausch MH, Herlitze S, Roth BL. 2007. Evolving the lock to fit the key to create a family of G protein-coupled receptors potently activated by an inert ligand. Proc Natl Acad Sci USA. 104:5163–5168.

Arnsten AF. 2009. Stress signalling pathways that impair prefrontal cortex structure and function. Nat Rev Neurosci. 10: 410–422.

Arnsten AF. 2015. Stress weakens prefrontal networks: molecular insults to higher cognition. Nat Neurosci. 18:1376–1385.

Barker GR, Bird F, Alexander V, Warburton EC. 2007. Recognition memory for objects, place, and temporal order: a disconnection analysis of the role of the medial prefrontal cortex and perirhinal cortex. J Neurosci. 27:2948–2957.

Cho JH, Deisseroth K, Bolshakov VY. 2013. Synaptic encoding of fear extinction in mPFC-amygdala circuits. Neuron. 80: 1491–1507.

Correll CM, Rosenkranz JA, Grace AA. 2005. Chronic cold stress alters prefrontal cortical modulation of amygdala neuronal activity in rats. Biol Psychiatry. 58:382–391.

Davidson RJ, Putnam KM, Larson CL. 2000. Dysfunction in the neural circuitry of emotion regulation–a possible prelude to violence. Science. 289:591–594.

de Kloet ER, Joëls M, Holsboer F. 2005. Stress and the brain: from adaptation to disease. Nat Rev Neurosci. 6:463–475.

Duffney LJ, Zhong P, Wei J, Matas E, Cheng J, Qin L, Ma K, Dietz DM, Kajiwara Y, Buxbaum JD, et al. 2015. Autism-like deficits in *Shank3*-deficient mice are rescued by targeting actin regulators. Cell Rep. 11:1400–1413.

Duman RS, Aghajanian GK. 2012. Synaptic dysfunction in depression: potential therapeutic targets. Science. 338:68–72.

Fortress AM, Hamlett ED, Vazey EM, Aston-Jones G, Cass WA, Boger HA, Granholm AC. 2015. Designer receptors enhance memory in a mouse model of down syndrome. J Neurosci. 35:1343–1353.

Garner AR, Rowland DC, Hwang SY, Baumgaertel K, Roth BL, Kentros C, Mayford M. 2012. Generation of a synthetic memory trace. Science. 335:1513–1516.

Gerhard DM, Wohleb ES, Duman RS. 2016. Emerging treatment mechanisms for depression: focus on glutamate and synaptic plasticity. Drug Discov Today. 21:454–464.

Gold PW. 2015. The organization of the stress system and its dysregulation in depressive illness. Mol Psychiatry. 20:32–47.

Goldman-Rakic PS. 1995. Cellular basis of working memory. Neuron. 14:477–485.

Hartmann J, Dedic N, Pöhlmann ML, Häusl A, Karst H, Engelhardt C, Westerholz S, Wagner KV, Labermaier C, Hoeijmakers L, et al. 2017. Forebrain glutamatergic, but not GABAergic, neurons mediate anxiogenic effects of the glucocorticoid receptor. Mol Psychiatry. 22:466–475.

Huang WC, Chen Y, Page DT. 2016. Hyperconnectivity of prefrontal cortex to amygdala projections in a mouse model of macrocephaly/autism syndrome. Nat Commun. 7:13421.

Kim SC, Jo YS, Kim IH, Kim H, Choi JS. 2010. Lack of medial prefrontal cortex activation underlies the immediate extinction deficit. J Neurosci. 30:832–837.

Krashes MJ, Koda S, Ye C, Rogan SC, Adams AC, Cusher DS, Maratos-Flier E, Roth BL, Lowell BB. 2011. Rapid, reversible activation of AgRP neurons drives feeding behavior in mice. J Clin Invest. 121:1424–1428.

Krueger DD, Osterweil EK, Chen SP, Tye LD, Bear MF. 2011. Cognitive dysfunction and prefrontal synaptic abnormalities in a mouse model of fragile X syndrome. Proc Natl Acad Sci USA. 108:2587–2592.

Lee JB, Wei J, Liu W, Cheng J, Feng J, Yan Z. 2012. Histone Deacetylase 6 gates the synaptic action of acute stress in prefrontal cortex. J Physiol. 590:1535–1546.

Li N, Liu RJ, Dwyer JM, Banasr M, Lee B, Son H, Li XY, Aghajanian G, Duman RS. 2011. Glutamate N-methyl-D-aspartate receptor antagonists rapidly reverse behavioral and synaptic deficits caused by chronic stress exposure. Biol Psychiatry. 69:754–761.

Liston C, McEwen BS, Casey BJ. 2009. Psychosocial stress reversibly disrupts prefrontal processing and attentional control. Proc Natl Acad Sci USA. 106:912–917.

López AJ, Kramár E, Matheos DP, White AO, Kwapis J, Vogel-Ciernia A, Sakata K, Espinoza M, Wood MA. 2016. Promoter-Specific Effects of DREADD Modulation on Hippocampal Synaptic Plasticity and Memory Formation. J Neurosci. 36:3588–3599.

Maffei A, Nelson SB, Turigiano GG. 2004. Selective reconfiguration of layer 4 visual cortical circuitry by visual deprivation. Nat Neurosci. 7:1353–1359.

Maffei A, Turigiano GG. 2008. Multiple modes of network homeostasis in visual cortical layer 2/3. J Neurosci. 28: 4377–4384.

Márquez C, Poirier GL, Cordero MI, Larsen MH, Groner A, Marquis J, Magistretti PJ, Trono D, Sandi C. 2013. Peripuberty stress leads to abnormal aggression, altered amygdala and orbitofrontal reactivity and increased prefrontal MAOA gene expression. Transl Psychiatry. 3:e216.

McDonald AJ. 1982. Neurons of the lateral and basolateral amygdaloid nuclei: a Golgi study in the rat. J Comp Neurol. 212:293–312.

Mcdonald AJ, Mascagni F, Guo L. 1996. Projections of the medial and lateral prefrontal cortices to the amygdala: a Phaseolus vulgaris leucoagglutinin study in the rat. Neuroscience. 71: 55–75.

McEwen BS. 2007. Physiology and neurobiology of stress and adaptation: central role of the brain. Physiol Rev. 87:873–904.

McEwen BS, Morrison JH. 2013. The Brain on Stress: Vulnerability and Plasticity of the Prefrontal Cortex over the Life Course. Neuron. 79:16–29.

Michaelides M, Anderson SA, Ananth M, Smirnov D, Thanos PK, Neumaier JF, Wang GJ, Volkow ND, Hurd YL. 2013. Whole-brain circuit dissection in free-moving animals reveals cell-specific mesocorticolimbic networks. J Clin Invest. 123: 5342–5350.

Popoli M, Yan Z, McEwen BS, Sanacora G. 2011. The stressed synapse: the impact of stress and glucocorticoids on glutamate transmission. Nat Rev Neurosci. 13:22–37.

Radley JJ, Rocher AB, Miller M, Janssen WG, Liston C, Hof PR, McEwen BS, Morrison JH. 2006. Repeated stress induces dendritic spine loss in the rat medial prefrontal cortex. Cereb Cortex. 16:313–320.

Ridderinkhof KR, Ullsperger M, Crone EA, Nieuwenhuis S. 2004. The role of the medial frontal cortex in cognitive control. Science. 306:443–447.

Rogan SC, Roth BL. 2011. Remote control of neuronal signaling. Pharmacol Rev. 63:291–315.

Rosenkranz JA, Grace AA. 2002. Cellular mechanisms of infralimbic and prelimbic prefrontal cortical inhibition and dopaminergic modulation of basolateral amygdala neurons in vivo. J Neurosci. 22:324–337.

Sanchez-Vives MV, McCormick DA. 2000. Cellular and network mechanisms of rhythmic recurrent activity in neocortex. Nat Neurosci. 3:1027–1034.

Savander V, Go CG, Ledoux JE, Pitkänen A. 1996. Intrinsic connections of the rat amygdaloid complex: projections originating in the accessory basal nucleus. J Comp Neurol. 374: 291–313.

Spampanato J, Polepalli J, Sah P. 2011. Interneurons in the basolateral amygdala. Neuropharmacology. 60:765–773.

Tielbeek JJ, Al-Itejawi Z, Zijlmans J, Polderman TJ, Buckholtz JW, Popma A. 2016. The impact of chronic stress during adolescence on the development of aggressive behavior: A systematic review on the role of the dopaminergic system in rodents. Neurosci Biobehav Rev. [Epub ahead of print].

Urban DJ, Roth BL. 2015. DREADDs (designer receptors exclusively activated by designer drugs): chemogenetic tools

with therapeutic utility. Annu Rev Pharmacol Toxicol. 55: 399–417.

Veenema AH, Blume A, Niederle D, Buwalda B, Neumann ID. 2006. Effects of early life stress on adult male aggression and hypothalamic vasopressin and serotonin. Eur J Neurosci. 24:1711–1720.

Wei J, Yuen EY, Liu W, Li X, Zhong P, Karatsoreos IN, McEwen BS, Yan Z. 2014. Estrogen protects against the detrimental effects of repeated stress on glutamatergic transmission and cognition. Mol Psychiatry. 19:588–598.

Wess J, Nakajima K, Jain S. 2013. Novel designer receptors to probe GPCR signaling and physiology. Trends Pharmacol Sci. 34:385–392.

Yau JO, McNally GP. 2015. Pharmacogenetic excitation of dorsomedial prefrontal cortex restores fear prediction error. J Neurosci. 35:74–83.

Yehuda R, LeDoux J. 2007. Response variation following trauma: a translational neuroscience approach to understanding PTSD. Neuron. 56:19–32.

Yuen EY, Liu W, Karatsoreos IN, Feng J, McEwen BS, Yan Z. 2009. Acute stress enhances glutamatergic transmission in prefrontal cortex and facilitates working memory. Proc Natl Acad Sci USA. 106:14075–14079.

Yuen EY, Liu W, Karatsoreos IN, Ren Y, Feng J, McEwen BS, Yan Z. 2011. Mechanisms for acute stress-induced enhancement of glutamatergic transmission and working memory. Mol Psychiatry. 16:156–170.

Yuen EY, Wei J, Liu W, Zhong P, Li X, Yan Z. 2012. Repeated stress causes cognitive impairment by suppressing glutamate receptor expression and function in prefrontal cortex. Neuron. 73:962–977.

Yuen EY, Zhong P, Li X, Wei J, Yan Z. 2013. Restoration of glutamatergic transmission by dopamine D4 receptors in stressed animals. J Biol Chem. 288:26112–26120.

Waltes R, Chiocchetti AG, Freitag CM. 2016. The neurobiological basis of human aggression: a review on genetic and epigenetic mechanisms. Am J Med Genet B Neuropsychiatr Genet. 171:650–675.

Zhong P, Yan Z. 2016. Distinct physiological effects of dopamine D4 receptors on prefrontal cortical pyramidal neurons and fast-spiking interneurons. Cereb Cortex. 21:62–70.